Journal of Photochemistry and Photobiology A: Chemistry 199 (2008) 303–310

Contents lists available at ScienceDirect

Journal of Photochemistry and Photobiology A: Chemistry

journal homepage: www.elsevier.com/locate/jphotochem

Kinetics of photochemical reactions in optically dense media with reagent diffusion

Andrey Kh. Vorobiev*, Denis Menshykau[1]

Moscow State University, Department of Chemistry, Leninskie Gory 1/3, GSP-2, 119991 Moscow, Russia

ARTICLE INFO

Article history:
Received 13 March 2008
Received in revised form 2 June 2008
Accepted 7 June 2008
Available online 17 June 2008

Keywords:
Optically dense media
Kinetics of photochemical reaction
Photochromic isomerization
Nonlinear kinetics
Diffusion kinetics

ABSTRACT

The kinetics of photochemical reactions in optically dense media with reagent diffusion is considered. It is shown, by example of the photochromic isomerization $A \leftrightarrow B$, that if the diffusion coefficient of A differs from the diffusion coefficient of B the disturbance of the initial uniform distribution of the total photochrome concentration $(A+B)$ along the light irradiation direction is observed. The greater the difference in diffusion coefficients, the greater the observed change in the total concentration distribution. The effect of change in total concentration along the light irradiation direction is found experimentally by the example of azobenzene dissolved in hydrogel and irradiated by UV light.

1. Introduction

The kinetics of photochemical reactions in optically dense media essentially free from diffusion has been examined in several papers [1–14]. A decrease in light intensity within the sample has been found to be a significant feature of such systems. The outermost layers absorb light significantly; therefore the light intensity and the photochemical reaction rate depend on the distance from the irradiated surface. As a result, the reagent as well as the reaction product concentrations is described by a wave-like distribution along the irradiation direction.

The kinetics of photochemical reactions in optically dense media was examined for photochrome undergoing purely photochemical transformation [1–12], and also in the presence of photochemical thermoreversible [13,14] reactions. We have previously considered kinetics of the photochromic transformation in optically dense media according to the scheme [14]:

$$A_1 \underset{h\nu,k}{\overset{h\nu,k}{\rightleftarrows}} A_2$$

It has been found that penetration of the wave into the sample is determined by thermal reaction rate constants. The wave shape is dependent on the ratio of the absorption coefficients of the initial and the product form of the photochrome and the ratio of quantum yields of photochemical reactions.

Until now, the influence of the diffusion mobility of reagents on photochemical reactions in optically dense media has not been examined. Meanwhile, it is well known that in reaction–diffusion systems involving feedback, a large variety of dissipative structures form [15–19], e.g. traveling waves, standing waves, helical and concentric waves and so on. The diffusion mobility of reagents may cause non-trivial kinetic behavior in significantly more simple systems as well. For example, unusual kinetics is observed in the reaction–diffusion process of type $A+B \rightarrow C$, with initially separated components [20–28].

Photochemical reactions in optically dense media with limited diffusion mobility take place in a variety of materials. Examples are systems for optical data storage, polymer under photodegradation, biological systems (photosynthesis, photodynamic therapy) and others. In all cases the distribution of light absorbing substances and products of photochemical transformations are important for quantitative description of processes.

Thus, the goals of this work are to consider theoretically the spatial distribution of reagents during the model photochemical isomerization reaction in an optically dense medium, taking into account the diffusion mobility and to verify experimentally the theoretical predictions.

* Corresponding author. Tel.: +7 495 9394900; fax: +7 495 9328846.
E-mail addresses: vorobiev@excite.chem.msu.ru (A.Kh. Vorobiev), dzianis.menshykau@sjc.ox.ac.uk (D. Menshykau).
[1] Moved to: University of Oxford, Department of Chemistry, Physical and Theoretical Chemistry Laboratory, South Parks Road, Oxford OX1 3QZ, UK. Tel.: +44 1865 275400; fax: +44 1865 275410.

1010-6030/$ – see front matter © 2008 Elsevier B.V. All rights reserved.
doi:10.1016/j.jphotochem.2008.06.004

2. Experimental and computational details

2.1. Chemicals

Gelatin "Sigma" G-2500 Type A, M_w = 80,000–120,000 was used without further purification. Commercial DMF, hexane and toluene were used without further purification.

cis-Azobenzene was obtained by following procedure: *trans*-azobenzene was dissolved in hexane and was irradiated 10 min with full light high-pressure mercury lamp with an intense stirring. Then the solution was additionally irradiated with light at wavelength λ = 313 nm. The reaction mixture was separated on the chromatographic column filled with Al_2O_3. *trans*-Azobenzene was eluted with hexane; *cis*-form was eluted with diethyl ester. The purity was controlled with chromatography on Silufol plates.

2.2. Sample preparation

Samples for photolysis in the absence of gel were prepared by dissolution of azobenzene in water/DMF mixture at 50 °C. The solution was filtered into a standard quarts UV–vis cell after cooling down.

Samples containing gelatin were prepared by following procedure: an exactly weighed quantity of gelatin was placed into quartz UV–vis cell with optical length l = 1 mm. In all samples the concentration of gelatin was no less than 5% weight. Azobenzene solution in water/DMF mixture was added to the cell. The gelatin was left for 3–5 h to swell and then the cell was heated to 40 °C. The solution was gently stirred and thermostated for several hours at 40 °C. Azobenzene distribution in the sample was measured after the cell was cooled to room temperature. If the difference in optical density between any points of the sample was more than 0.03D, the procedure of heating and thermostating was repeated. After a smooth azobenzene distribution was reached, the change of distribution was measured for 24 h. The sample was used for photolysis if distribution did not change during the day.

2.2.1. Parameters measurement of the system azobenzene in water/DMF mixture

UV–vis spectra were recorded using a Shimadzu UV 2401 PC spectrometer or a Carl Zeiss Specord M40 spectrometer. To measure extinction coefficients, a preweighed quantity of azobenzene was dissolved in an aliquot of water/DMF mixture. The optical density at wavelength λ = 436 nm was 0.5–0.7D in a cell with optical path length l = 1 mm. An Aliquot of this solution was placed into a cell with optical path length 5, 10, 20, 30, 50 mm and was diluted with an exactly measured quantity of water/DMF mixture to keep constant optical density. Azobenzene absorption spectra were improved by subtraction of the absorption spectrum of water/DMF mixture recorded in the same cell.

The azobenzene *cis* → *trans* isomerization was monitored by the change in absorbance using a cell with optical length l = 1 mm and l = 10 mm.

A high-pressure mercury lamp (500 W) was used as a light source. A parallel light beam was formed with system of quarts lenses. The standard glassy filters were used for isolation of narrowband radiation.

The cells were irradiated in two ways: in side (Fig. 1(a)) and cell-end (Fig. 1(b)). Before irradiation the cell-end was polished until optical transparence was achieved. The light intensity at wavelength λ = 365 nm was determined by ferryoxalate actinometry [40]. The light intensities were 2.4×10^{16} photon/(s sm^2) on irradiation into side and 2.9×10^{16} photon/(s sm^2) on irradiation into cell-end. Measurements were carried out in quarts cells in the condition similar to azobenzene photolysis.

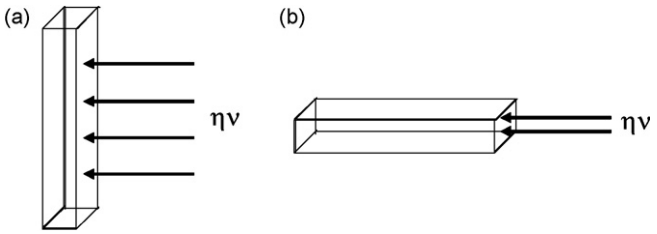

Fig. 1. Cell irradiation into side (a) and cell-end (b).

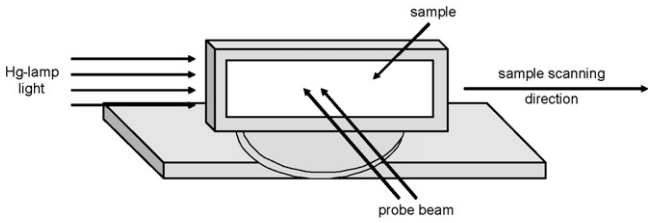

Fig. 2. Scheme of the device for azobenzene distribution measurement.

The cell was fixed in a holder (Fig. 2) for azobenzene distribution measurements. Optical density was measured on the spectrometer Specord M40, probe beam direction was perpendicular to irradiation light from the mercury lamp. The intensity of probe beam is negligible in comparison with intensity of Hg-lamp. The sample was moved in 0.1 mm steps relative to the probe beam.

2.3. Numerical integration of differential equation system

The system of differential equations (2) was solved by an explicit finite difference method with variable time step (see supplementary data III).

3. Results and discussion

3.1. Theoretic consideration

Let us consider the photochrome undergoing direct thermal and photochemical reactions, as well as reverse thermal and photochemical reactions in agreement with the scheme:

$$A_1 \underset{h\nu,k}{\overset{h\nu,k}{\rightleftarrows}} A_2$$

taking into account diffusion mobility of compounds A_1 and A_2. In this case, the photochemical reaction $A_1 \rightarrow A_2$ proceeds when the sample is irradiated. The photochrome exists in form A_2 near the irradiated surface and stays in form A_1 in the bulk of the sample. Under these circumstances A_2 diffuses from the outer surface of the sample into the bulk, while A_1 diffuses from the bulk to the outer surface. Photochrome forms A_1 and A_2 have different structures and because of this they have different diffusion coefficients. As a result the diffusive flow of substance A_1 differs from the diffusive flow of A_2, and the total concentration $(A_1 + A_2)$ change will take place along the irradiation direction. We will name this effect photoconcentration.

The photochrome distribution in the sample is described by the system of differential equations (1). The first equation is the Beer–Lambert law in a differential form; the following equations describe photochemical and thermal transformations, as well as

diffusion.

$$\begin{aligned}\frac{\partial I}{\partial l} &= -I(\varepsilon_1 A_1 + \varepsilon_2 A_2)\\ \frac{\partial A_1}{\partial t} &= -\phi_1\varepsilon_1 I A_1 + \phi_2\varepsilon_2 I A_2 - k_1 A_1 + k_2 A_2 + D_1\frac{\partial^2 A_1}{\partial l^2}\\ \frac{\partial A_2}{\partial t} &= \phi_1\varepsilon_1 I A_1 - \phi_2\varepsilon_2 I A_2 + k_1 A_1 - k_2 A_2 + D_2\frac{\partial^2 A_2}{\partial l^2}\end{aligned} \quad (1)$$

where $I(x, t)$ is the light intensity; $A_1(x, t)$, $A_2(x, t)$ are the concentration of the substances; ε_1, ε_2, D_1, and D_2 are the extinction coefficients and diffusion coefficients of substances A_1 and A_2, respectively; ϕ_1 and ϕ_2 are the quantum yields of $A_1 \rightarrow A_2$ and $A_2 \rightarrow A_1$ reactions, respectively; k_1 and k_2 are the constants of thermal monomolecular reactions $A_1 \rightarrow A_2$ and $A_2 \rightarrow A_1$, respectively.

Initial and boundary conditions can be written as follows: $A_1(l, 0) = k_2/(k_1 + k_2)$, $A_2(l, 0) = k_1/(k_1 + k_2)$, if uniform distribution is assumed at the initial time and $I(0, t) = I^0$, $\partial A_i/\partial l(0, t) = 0$; $\partial A_i/\partial l(l^0, t) = 0$, where l^0 is the length of the sample.

Next, dimensionless variables and parameters were applied

$A = A_1/A_1^0 + A_2^0$, $B = A_2/A_1^0 + A_2^0$ is the dimensionless concentrations; $i = I/I^0$ is the dimensionless light intensity; $\tau = t\phi_1\varepsilon_1 I^0$ is the dimensionless time; $x = l\varepsilon_1({A_1}^0 + {A_2}^0)$ is the dimensionless space coordinate; $x = l^0\varepsilon_1({A_1}^0 + {A_2}^0)$ is the dimensionless length of the sample; $\gamma_i = \kappa_i/\phi_1\varepsilon_1 I^0$ is the dimensionless thermal rate constant; $\alpha = \varepsilon_2/\varepsilon_1$ is the absorption coefficients ratio; $\beta = \phi_2/\phi_1$ is the quantum yield ratio; $D_A = \left(A_1^0 + A_2^0\right)\varepsilon_1 D_1/\left(\phi_1\varepsilon_1 I^0\right)$; $D_B = \left(A_1^0 + A_2^0\right)\varepsilon_1 D_2/\left(\phi_1\varepsilon_1 I^0\right)$ is the dimensionless diffusion coefficients. Here, $A_i^0 = A_1(1, 0)$ is the concentration of A_i at the initial time.

The PDE system (1) can be written in dimensionless variables

$$\begin{aligned}\frac{\partial i}{\partial x} &= -\mathrm{i}(A + \alpha A)\\ \frac{\partial A}{\partial \tau} &= -\mathrm{i}A + \alpha\beta B - \gamma_1 A + \gamma_2 B + D_A\frac{\partial^2 A}{\partial x^2}\\ \frac{\partial B}{\partial \tau} &= \mathrm{i}A - \alpha\beta B + \gamma_1 A - \gamma_2 B + D_B\frac{\partial^2 B}{\partial x^2}\end{aligned} \quad (2)$$

Boundary and initial conditions are

$$A(x, 0) = \frac{\gamma_2}{(\gamma_1 + \gamma_2)}; \quad B(x, 0) = \frac{\gamma_1}{(\gamma_1 + \gamma_2)}; \quad i(0, \tau) = 1;$$

$$\left.\frac{\partial A}{\partial x}\right|_{0,\tau} = 0; \quad \left.\frac{\partial B}{\partial x}\right|_{0,\tau} = 0; \quad \left.\frac{\partial A}{\partial x}\right|_{x_0,\tau} = 0; \quad \left.\frac{\partial B}{\partial x}\right|_{x^0,\tau} = 0, \quad (3)$$

where

$$x_0 = \varepsilon_1(A_1^0 + A_2^0)l_0$$

Since the PDE system (2) has no exact solution, some particular cases are examined below.

3.1.1. Equal diffusion coefficients

In the case of equal diffusion coefficients $D_B = D_A$ photochrome distribution in the sample is even during the whole irradiation time (supplementary data I).

3.1.2. Concentration distribution at infinitely long irradiation

The system reaches the stationary state and the concentrations are constant in time as $\tau \rightarrow \infty$. It can be proved that uneven photochrome distribution are achieved at prolonged light irradiation when $D_A \neq D_B$ (see supplementary data II). Concentration A near the irradiated surface in the stationary state is ordinary less than in the bulk as a result of photochemical reaction. If $D_A < D_B$ then the total concentration $A + B$ in the beginning of the sample in this stationary state is less than in the bulk (see supplementary data II). If $D_A > D_B$, then the total concentration $A + B$ in the beginning of the sample is higher than in the bulk. The larger the absolute ratio of diffusion coefficients, the larger the coefficient of linear dependence, and the larger the photoconcentration effect. In paper [14] it was shown that at certain parameter values, concentration A near the front surface could be higher than in the bulk. This case can be reduced to the previous one by swapping photochrome forms in the equations.

Let us consider the next particular case, where only one form of the photochrome can diffuse: $D_A \neq 0$; $D_B = 0$. The concentration profiles for this case can be obtained from (see supplementary data II):

$$A(x) = \frac{c}{D_A}; \quad B(x) = \left[\frac{1}{\gamma_2}\exp\left(-\frac{c}{D_A}x\right) + \frac{\gamma_1}{\gamma_2}\right]\frac{c}{D_A} \quad (4)$$

where the constant c can be found from the transcendental equation

$$\frac{\gamma_1 + \gamma_2}{\gamma_2}\frac{c}{D_A}x_0 + \frac{1}{\gamma_2}\left[1 - \exp\left(-\frac{c}{D_A}x\right)\right] = x_0 \quad (5)$$

The distribution of the total concentration of the photochrome in the stationary state calculated from expressions (4) and (5) at different values of γ_2 (dimensionless thermal rate constant of the reverse reaction), is presented in Fig. 3.

Fig. 3(a) shows that effect of photoconcentration achieves a maximum as the rate of the thermal reaction changes. The largest photoconcentration effect is reached at $\gamma_2 \approx 0.1$. The requirement for the observation of an uneven distribution in the stationary state is the presence of thermal reactions. Indeed, it can be verified by direct substitution into equations that in the absence of thermal reactions, $\gamma_1 = \gamma_2 = 0$, the stationary distribution of photochrome becomes uniform and is given by expression (4):

$$A(x) = \frac{\alpha\beta}{\alpha\beta + 1}; \quad B(x) = \frac{1}{\alpha\beta + 1} \quad (6)$$

Fig. 3(b) shows distribution of forms A and B in the sample. A is distributed evenly in the sample, that is a common case than one of the photochrome forms has diffusion coefficient equal to zero. At low values of the rate of the reverse thermal reaction γ_2 gradient of photochrome form B is proportional to γ_2, however, the higher the rate of thermal back reaction γ_2 the less concentration of form B is observed in the sample. Consequently, the quantity of substance deviated from equilibrium passes through the maximum on γ_2 increase.

For a quantitative description of the photoconcentration effect, let us introduce the extent of photoconcentration χ as the ratio of the quantity of substances $A_1 + A_2$ shifted from uniform distribution to the total quantity of substance in the sample

$$\chi = \frac{1}{2x_0}\int_0^{x_0} |A + B - 1|\mathrm{d}x \quad (7)$$

According to this definition, the extent of photoconcentration in a sample with even distribution is zero, but in a sample with distribution described by the delta function is one. In all cases the extent of photoconcentration is lies between zero and one.

The extents of photoconcentration at various values γ_1, γ_2 and x_0 in the stationary state are presented in Fig. 4. The highest extent of photoconcentration is achieved in the absence of the direct thermal reaction $\gamma_1 = 0$ (Fig. 4(a)). The maximal extent photoconcentration, in the considered particular case ($D_B = 0$, $\alpha = 0$), is observed at $x_0\gamma_2 = 1$ (Fig. 4(b)).

Analytical solution for more general case $D_B = 0$, $\alpha \neq 0$ is given in supplementary data II, here we just notice that reagents distribution does not depend on diffusion coefficient D_A.

In the general case, solution in reagents distribution in stationary state can be found only numerically. Distribution of the total concentration ($A + B$) and concentration of form A in the stationary

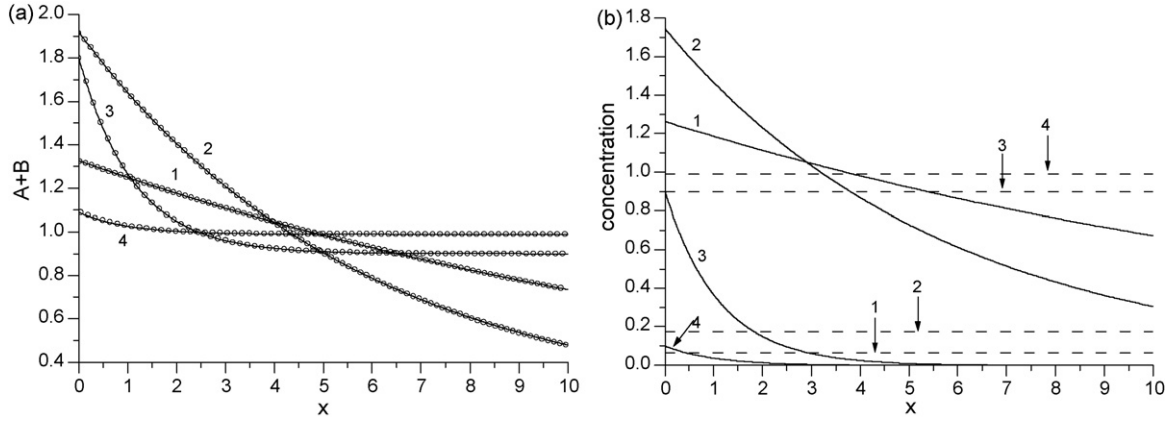

Fig. 3. (a) Distribution of the total concentration ($A+B$) in the sample in stationary state. Results of analytical and numerical solutions are presented in solid and scattered lines, respectively. (b) Distribution of the A—dashed line and B—solid line in the sample in stationary state. $D_B = 0$, $\alpha = 0$, $\gamma_1 = 0$, $x^0 = 10$; 1, $\gamma_2 = 0.05$; 2, $\gamma_2 = 0.1$; 3, $\gamma_2 = 1$; 4, $\gamma_2 = 10$.

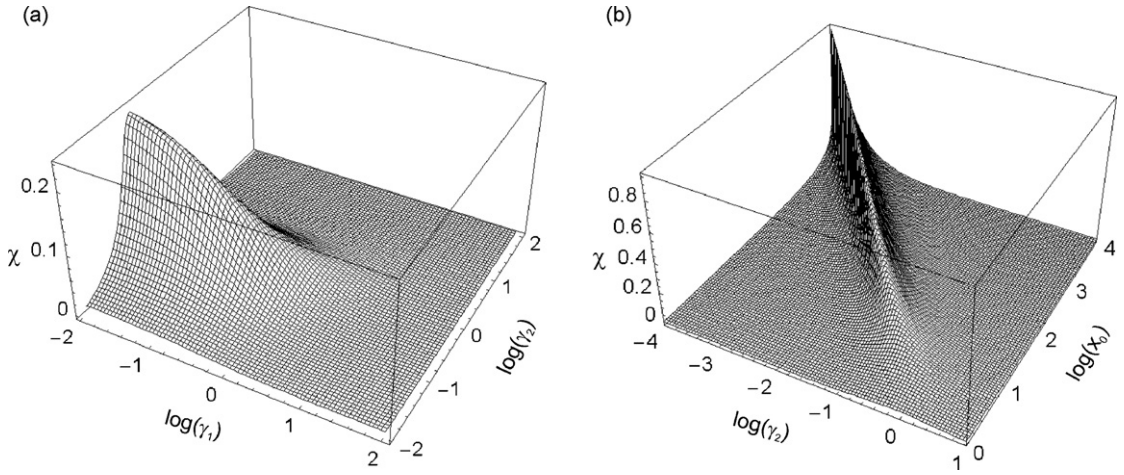

Fig. 4. (a) Extent of photoconcentration χ at various values of parameters γ_1 and γ_2; $x_0 = 10$. (b) Extent of concentration χ at various values of parameters γ_2 and x_0; $\gamma_1 = 0$, $D_B = 0$, $\alpha = 0$ for both cases (a) and (b).

state at various values of diffusion coefficient ratio D_A/D_B is presented in Fig. 5. It is seen that the larger the difference between diffusion coefficients, the larger the deviation of total concentration from uniformity (Fig. 5(a)). If $D_A > D_B$ photoconcentration is observed near the irradiated surface, if $D_A < D_B$, photoconcentration is observed in the bulk of the sample. This result is in agreement with analytical results, presented in supplementary data II. Form A or B are distributed almost evenly (Fig. 5(b)) when the ratio D_A/D_B is high or low accordingly. These results are in agreement with analytical predictions (4).

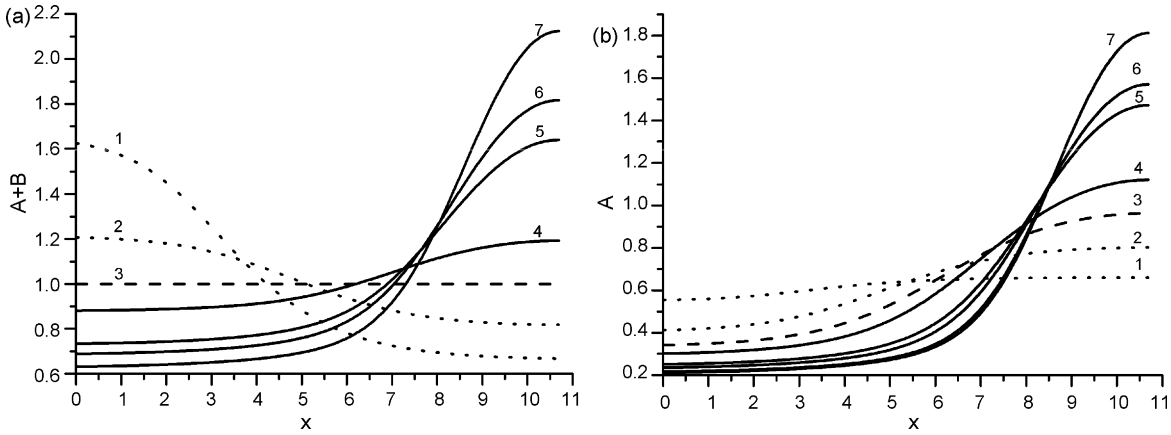

Fig. 5. Stationary distribution of the total concentration ($A+B$) (a) and concentration of form A (b) at various values of ratio D_A/D_B: 10 (1); 5 (2); 1 (3); 0.62 (4); 0.31 (5); 0.16 (6); 0.036 (7). Other parameters have next values: $\alpha = 0.5$; $\beta = 1$; $\gamma_1 = 0$; $\gamma_2 = 0.018$; $D_A = 0.018$; $x^0 = 10.7$.

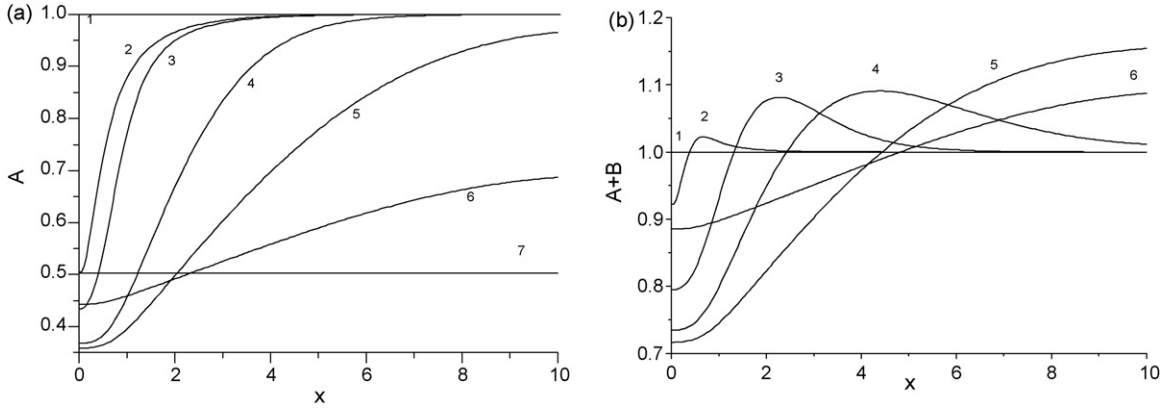

Fig. 6. Distribution of the concentration A (a) and the total concentration $(A+B)$ (b) in the sample at different values of dimensionless irradiation time $\tau = 0$ (1); $\tau = 20$ (2); $\tau = 400$ (3); $\tau = 2000$ (4); $\tau = 10{,}000$ (5); $\tau = 40{,}000$ (6); $\tau = +\infty$ (7, a) and (1, b). The following parameters values were used for modeling: $\alpha = 0.5$; $\beta = 1$; $\gamma_1 = 0$; $\gamma_2 = 0$; $D_A = 0.029$; $D_B = 0.00058$; $x^0 = 10$.

The presented analysis shows, that uneven distribution of photochrome (photoconcentration effect) can be observed when the photochrome undergoes photochemical reaction in optically dense media, and when the photochrome forms have different diffusion coefficients. In the stationary state, which is reached at infinitely long irradiation of the sample, photoconcentration is observed only when thermal isomerization reactions are presented. The degree of photoconcentration depends non-monotonic on parameters values. Analysis of stationary states, however, cannot give any information about kinetic processes. Consequently, numerical modeling of the processes must be performed.

3.1.3. Numerical solution of the system (2)

Let us first consider the reaction of photochemical isomerization in optically dense media in the absence of thermal reactions. The results of numerical calculations for this particular case are presented in Fig. 6. One can see from Fig. 6(a) that at irradiation times $\tau \sim 20$, a decrease in the concentration A of the initial photochrome form is observed near the irradiated surface. Fig. 6(b) demonstrates, that a decrease in the total concentration $(A+B)$ near the front surface and an increase of the total concentration in the bulk are observed on irradiation of the sample. On prolonged irradiation, reaction wave penetrates deeper into the sample (Fig. 6(a)) and the photoconcentration effect increases. Maximal concentration deviation from uniform distribution is observed at dimensionless time $\tau \sim 10{,}000$.

Fig. 6(b) shows, that at $\tau = 40{,}000$ the degree of photoconcentration decreases and at $\tau = 200{,}000$ the distribution of $(A+B)$ again becomes uniform. This observation is in good agreement with the qualitative results shown in the previous section. In fact, in the absence of thermal isomerization reactions, photochrome form distributions in the sample in the stationary state are given by Eq. (6). This expression shows that distribution of photochrome forms along the direction of light propagation is uniform, and the ratio of photochrome forms A/B is equal to that for a photochemical reaction in an infinitely fine layer. Accordingly, in the absence of the thermal reaction, photoconcentration is observed only temporarily (Fig. 7(b)).

If the thermal reaction of isomerization is taken into account, system behavior is qualitatively similar to that described above. Results of numerical modeling for this case are presented in Fig. 7(a). It is seen that a decrease in total concentration $(A+B)$ near the irradiated surface and an increase in $(A+B)$ in the bulk of sample are also observed during photochemical reaction. However, photoconcentration does not disappear in the stationary state. This result is in agreement with theoretical predictions. Indeed, it was shown analytically above that in the presence of thermal reactions substance is distributed unevenly in the stationary state.

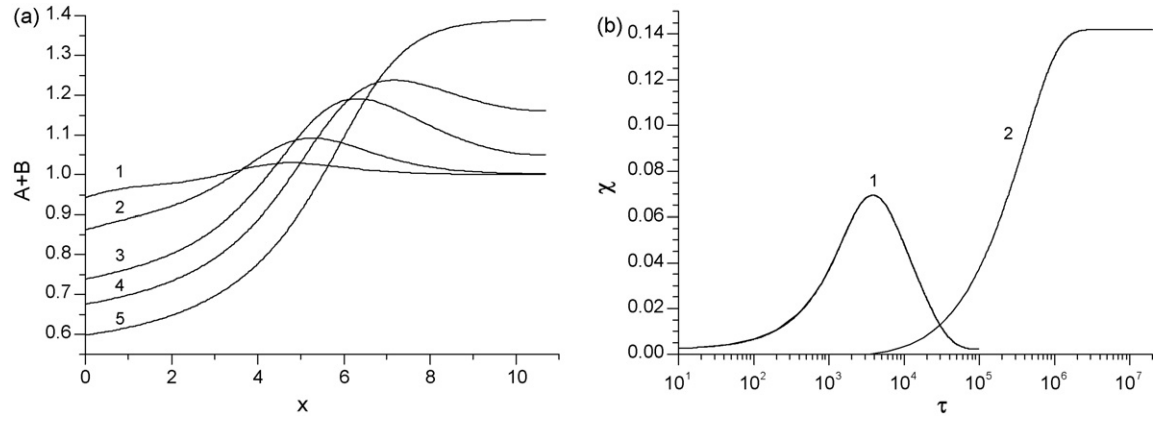

Fig. 7. (a) The distribution of the total concentration $(A+B)$ at different values of the dimensionless irradiation time: $\tau = 1.6 \times 10^3$ (1); 6.4×10^3 (2); 12.8×10^3 (3); 100×10^3 (4); 800×10^3 (5). Following values of dimensionless parameters were used for modeling: $\alpha = 0.5$; $\beta = 1$; $\gamma_1 = 0$; $\gamma_2 = 0.18$; $D_A = 0.00018$; $D_B = 0.00058$; $x^0 = 10$. (b) The change of photoconcentration value χ during irradiation of the sample. The following values of dimensionless parameters were used for modeling: (1) $\alpha = 0.5$; $\beta = 1$; $\gamma_1 = 0$; $\gamma_2 = 0$; $D_A = 0.029$; $D_B = 0.00058$; $x^0 = 10$; (2) $\alpha = 0.5$; $\beta = 1$; $\gamma_1 = 0$; $\gamma_2 = 0.18$; $D_A = 0.00018$; $D_B = 0.00058$; $x^0 = 10$.

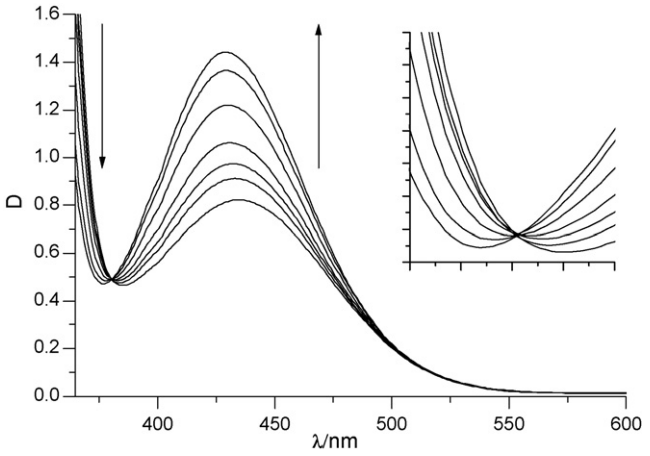

Fig. 8. Absorption spectra of azobenzene in water:DMF = 45:55 mixture on irradiation with light at wavelength λ = 365. Irradiation time is: 0, 0.5, 1, 2, 4, 6, 9 min.

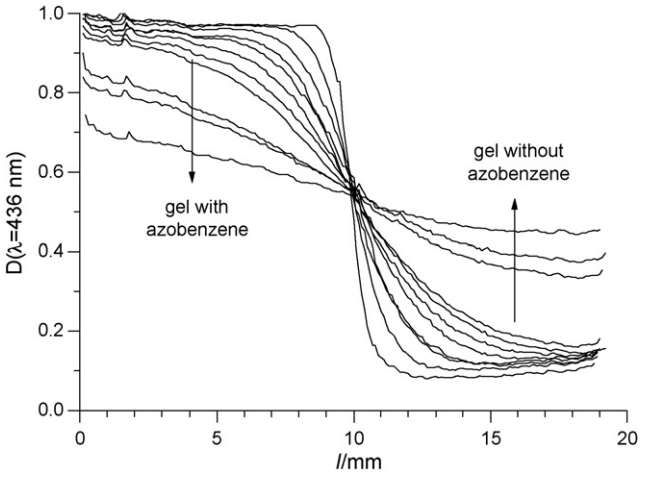

Fig. 9. *trans*-Azobenzene diffusion from gel with the dye into clear one. t = 0, 0.38, 1.1, 1.6, 2.5, 3.8, 5.2, 6.7, 17.2, 30.3, 50.4 h.

3.2. Experimental results and discussion

In order to experimentally verify the photoconcentration effect, a solution of azobenzene in gel water/dimethylformamide (DMF)/gelatin was used. Azobenzene was used as a photochrome, since it undergoes reactions of *cis* → *trans* and *trans* → *cis* photoisomerization reactions [29–34]. It is known that *cis*-azobenzene undergoes thermal isomerization into the *trans*-form. The rate of thermal isomerization depends on pH and solvent [35,36]. The geometry and polarity of the molecule are changed dramatically on isomerization [37]. Consequently, different diffusion coefficients should be expected for the *cis*- and *trans*-forms of azobenzene. A gel of water/DMF/gelatin was used to prevent convection, since gelatin is optically transparent and stable to UV irradiation [38]. DMF was added to system to increase the solubility of azobenzene.

3.2.1. Parameters of system azobenzene in mixture water/DMF

Absorption coefficients of azobenzene in the examined system are $\varepsilon_{cis}(\lambda = 365\,\text{nm}) = 420\,\text{dm}^3\,\text{mol}^{-1}\,\text{cm}^{-1}$, $\varepsilon_{cis}(\lambda = 436\,\text{nm}) = 1100\,\text{dm}^3\,\text{mol}^{-1}\,\text{cm}^{-1}$ and $\varepsilon_{trans}(\lambda = 365\,\text{nm}) = 1600\,\text{dm}^3\,\text{mol}^{-1}\,\text{cm}^{-1}$; and $\varepsilon_{trans}(\lambda = 436\,\text{nm}) = 710\,\text{dm}^3\,\text{mol}^{-1}\,\text{cm}^{-1}$. It was found that the absorption coefficient near $\lambda \sim 430$ nm depends on the dye concentration for *trans*-azobenzene. If concentration of the dye increases five times absorption coefficient decreases by ~10%.

trans-Azobenzene isomerizes into *cis*-azobenzene (Fig. 8) on irradiation with light at wavelength λ = 365 nm. Optical density increases near absorption band $\lambda \sim 430$ nm, and the isosbestic point is observed at wavelength λ = 381 nm when the system is irradiated with light at wavelength λ = 365 nm for a short time (Fig. 8). At longer irradiation times the isosbestic point is not observed any more, and optical density decrease slightly at wavelength λ = 430 nm. Isomerization is not observed in freshly prepared solutions of *cis*- and *trans*-azobenzene in water/DMF solution on irradiation with light at wavelengths λ = 436 nm and λ = 405 nm, whereas fast photoisomerization at both wavelengths is observed if the solution was preliminarily irradiated with light at wavelength λ = 365 nm.

The kinetics of the thermal *cis* → *trans* isomerization is described by the first-order kinetic law. The half-life is a several days if the sample is prepared by dissolution of pure *cis*-azobenzene in water:DMF = 55:45 mixture. However, when the azobenzene solution is irradiated with light atλ = 365 nm, time of half-life of the *cis* → *trans* isomerization becomes equal to 4 min.

Results presented above show that in system water/DMF/azobenzene the absorption spectra depend on concentration; the rate of thermal isomerization and quantum yields of photochemical isomerization depend on irradiation time with light at wavelength λ = 365 nm. These experimental facts are, apparently, evidence of the formation of an azobenzene associate in the examined system. Obviously, the ability of azobenzene to take part in photochemical and thermal reactions in associates differs significantly from those in true solutions. Azobenzene associates, apparently, decompose on irradiation with light λ = 365 nm.

Quantum yields of photochemical reactions were determined by a procedure described in [30], subject to the condition that thermal isomerization can be neglected. Quantum yields of azobenzene isomerization on irradiation with light λ = 365 nm are equal to $\phi = 0.13 \pm 0.005$ for *trans* → *cis* and $\phi = 0.44 \pm 0.01$ for *cis* → *trans* transformations. These values of quantum yield are in good agreement for those in non-polar solvents [34,39], e.g. quantum yields of isomerization in isooctane are $\phi = 0.12$ and $\phi = 0.48$, respectively.

The following experiments were made for the determination of the diffusion coefficients of *trans*- and *cis*-azobenzene in gel which consists of water:DMF = 45:55 mixture and 5 wt% of gelatin. The layer of gel with azobenzene was brought into contact with the layer of gel without the dye. Next, optical density profiles were registered along such composite sample during time. The *trans*-azobenzene distribution in the sample at different moments in time is presented in Fig. 9.

The gradient of azobenzene concentration in the middle of the sample is calculated from experimentally registered concentration profiles. The value of this concentration gradient during such an experiment is described by formula (8), which is obtained from diffusion equation solution by the Fourier series method

$$k(t) = \frac{l_0}{C^0}\frac{\partial C}{\partial l}(0,t) = -2\sum_{i=1}^{+\infty}\exp\left[-\pi^2(2k+1)^2\frac{D_c}{l_0^2}t\right] \quad (8)$$

Expression (8), with empirical correction t_0 to time t, was used to approximate experimental data. The correction is introduced to take into account some mixing of layers during bringing into contact of last. The number of term, in expression (8) was chosen so that addition of extra terms does not change diffusion coefficients more than experimental error. The diffusion coefficients for *cis*- and *trans*-azobenzene amount to $(3.1 \pm 0.2) \times 10^{-10}$ and $(4.5 \pm 0.2) \times 10^{-10}$ m^2/s correspondingly.

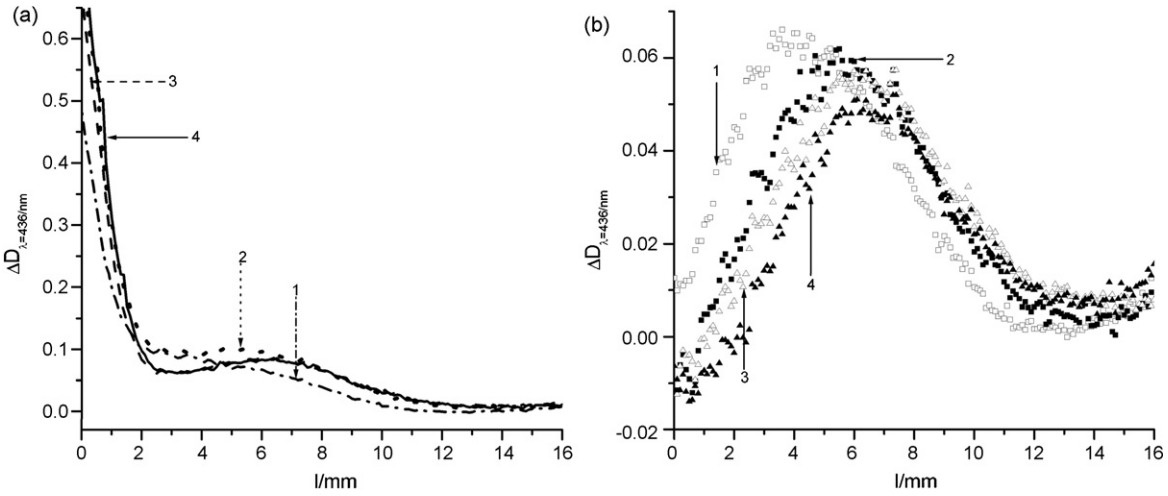

Fig. 10. Distribution of optical density (λ = 436 nm) in the sample along the light irradiation direction (λ = 365 nm) (a) immediately after irradiation and (b) after thermal *cis* → *trans*-azobenzene isomerization. At both (a) and (b) 1, *t* = 1.2 h; 2, *t* = 4.2 h; 3, *t* = 8.4 h; 4, *t* = 12 h.

3.2.2. Photochemical isomerization of azobenzene in optically dense media

A sample with high optical density containing azobenzene in gel was irradiated with light at wavelength λ = 365 nm. The optical density distribution in the sample along the light irradiation direction is presented in Fig. 10(a). It is seen that optical density increases near the irradiated surface. Consequently, *trans*-azobenzene isomerizes into the *cis*-form. In the bulk of the sample (3–8 mm from irradiated surface), an increase of optical density is also observed. Light cannot penetrate to such depth at the azobenzene concentration used. Consequently, the increase in optical density is explained by *cis*-azobenzene diffusion into the bulk of the sample.

To discover photoconcentration, the sample was stored in darkness for the time necessary for thermal *cis* → *trans* azobenzene isomerization. Afterwards sample was scanned along the light irradiation direction to determine photochrome distribution in the sample. Results of these measurements are presented in Fig. 10(b). It is clearly seen that the increase of optical density in the bulk of the sample is observed. In the course of irradiation the maximum of optical density moves into the bulk of the sample; such behavior is in agreement with theoretical predictions. Results of the modeling of the process using the parameters experimentally determined above are presented in Fig. 11. Comparison of Figs. 11 and 10 shows that experimental data are in semi-quantitative agreement with the results of modeling. From these figures it is also seen, that the decrease of optical density near the irradiated surface is significantly less than one predicted theoretically. Such a difference between theory and experiment should be explained by fact that azobenzene associates occur in real samples. Association was not taken into account in the theoretical model. Absorption coefficient of azobenzene in associates is less than for free azobenzene molecules. It was shown above that azobenzene associates are destroyed under irradiation with light at wavelength 365 nm. In that case azobenzene in the front part of the sample is non-associated, resulting in higher optical density than predicted theoretically.

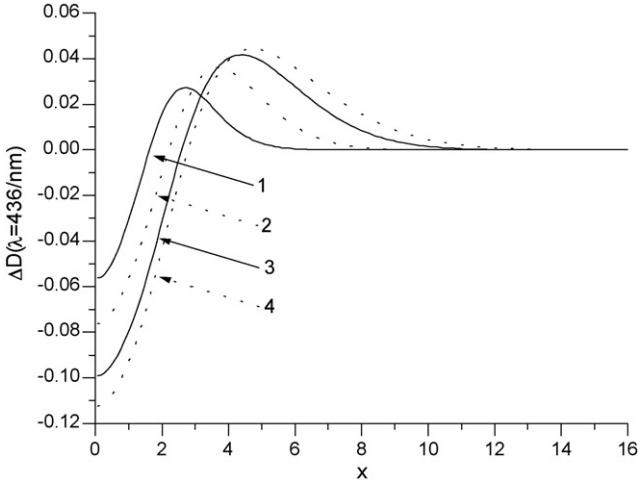

Fig. 11. Modeling of azobenzene photoconcentration with parameters values determined experimentally. (1) *t* = 1.2 h; (2) *t* = 4.2 h; (3) *t* = 8.4 h; (4) *t* = 12 h.

4. Conclusions

It has been shown, that light intensity distribution in optically dense media can cause pattern formation, if photochemically active molecules have diffusion mobility. It was found experimentally that in the course of photochemical isomerization of azobenzene in gel the dye concentration increases in the bulk of the sample and decreases near the irradiated surface. Theoretically it was shown that such a photoconcentration effect should be observed when the photochemical reaction take place in optically dense media, and reagents have diffusion mobility. The larger the difference in diffusion coefficients between initial compound and the photoproduct, the larger the observed photoconcentration effect.

Acknowledgement

This work was supported by the Russian Foundation for Base Research Project No. 06-03-32231.

Appendix A. Supplementary data

Supplementary data associated with this article can be found, in the online version, at doi:10.1016/j.jphotochem.2008.06.004.

References

[1] V.M. Treushnikov, A.M. Yanin, Zhurnal Nauchnoi i Prikladnoi Fotografii i Kinematografi (J. Pure Appl. Photogr. Kinetmatogr.) 32 (1987) 161.

[2] R.F. Davletshin, N.N. Kudryavtsev, O.V. Yatsenko, Kinetica i cataliz (Kinet. Catal.) 34 (1993) 780.
[3] V.V. Ivanov, B.L. Rytov, V.B. Ivanov, Polym. Sci. A 40 (1998) 1.
[4] A. Vorob'ev, Kh. Gurman, V.S. Khimia, Visokix energiy (High Energy Chem.) 19 (1985) 148.
[5] B.D. Gupta, I.C. Goyal, J. Photochem. 30 (1985) 173.
[6] J.R. Sheats, J.J. Diamond, J.M. Smith, J. Phys. Chem. 92 (1988) 4922.
[7] B.W. Darwell, J. Chem. Soc., Faraday Trans. 81 (1985) 1647.
[8] S. Ducharme, J. Hautala, P.C. Taylor, Phys. Rev. B 41 (1990) 12250.
[9] H. Mauser, Z. Naturforsch C 34 (1979) 1264.
[10] H. Mauser, Z. Naturforsch C 34 (1979) 1295.
[11] H. Mauser, Z. Naturforsch B 22 (1967) 569.
[12] R. Trabitzsch, J. Epperlein, Zeit. Chem. 16 (1976) 458–459.
[13] V.I. Babushok, S.S. Minaev, I.G. Namyatov, Combust. Explosion Shock Waves 32 (1996) 386.
[14] A. Vorobiev, D. Menshykau, J. Photochem. Photobiol. A: Chem. 197 (2008) 359–363.
[15] R.J. Field, M. Burger, Oscillations and Traveling Waves in Chemical Systems, Wiley–Interscience, 1985.
[16] A.F. Taylor, Prog. Reaction Kinet. Mech. 27 (2002) 243.
[17] A.M. Zabotinskiy, Concentration Autooscillations, Nauka, Moscow, 1974.
[18] A.S. Mikhailov, K. Showalter, Phys. Rep. 425 (2006) 79.
[19] V.K. Vanag, Phys.-Uspekhi 47 (2004) 923.
[20] L. Galfi, Z. Racz, Phys. Rev. A 38 (1988) 3151.
[21] H. Taitelbaum, L. Koo, Shl. Havlin, R. Kopelman, G. Weiss, Phys. Rev. E 46 (1992) 2151.
[22] S. Park, H. Peng, R. Kopelman, H. Taitelbaum, Phys. Rev. E 75 (2007) 026107.
[23] Zb. Koza, H. Taitelbaum, Phys. Rev. E 54 (1996) R1040–R1043.
[24] S. Park, S. Parus, R. Kopelman, H. Taitelbaum, Phys. Rev. E 64 (2001) 55102.
[25] H. Taitelbaum, A. Yen, R. Kopelman, Shl. Havlin, G. Weiss, Phys. Rev. E 54 (1996) 5942.
[26] I. Hecht, H. Taitelbaum, Phys. Rev. E 74 (2006) 012101.
[27] Z. Koza, H. Taitelbaum, Phys. Rev. E 56 (1997) 6387.
[28] I. Hecht, Y. Moran, H. Taitelbaum, Phys. Rev. E 73 (2006) 051109.
[29] A.V Elcov, Organicheskie Photochromi (Organic Photochromes), Ximia, Leningrad, 1982.
[30] V. Barachevskiy, G. Lashkov, V. Cexomskiy, Photochromism i ego primenenie (Photochromism and Its Application), Ximia, Moscow, 1977.
[31] G.E. Lewis, J. Org. Chem. 25 (1960) 2193.
[32] T. Fujino, Yu.S. Arzhantsev, T. Tahara, J. Phys. Chem. A 105 (2001) 8123.
[33] T. Saito, T. Kobayashi, J. Phys. Chem. A 106 (2002) 9436.
[34] G. Zimmerman, L. Chung, U. Paik, J. Am. Chem. Soc. 80 (1958) 3528.
[35] S. Hartley, J. Chem. Soc. (1938) 633.
[36] P. Bortolus, S. Monti, J. Phys. Chem. 83 (1979) 648.
[37] J.J. DeLang, J.M. Reobertson, S. Woodward, Proc. R. Soc. London, Ser. A 171 (1939) 398.
[38] A. Sionkowskaa, M. Wisniewski, J. Skopinska, C. Kennedy, T. Wess, J. Photochem. Photobiol. A: Chem. 162 (2004) 545.
[39] G. Gauglitz, S. Hubig, J. Photochem. 30 (1985) 121.
[40] K.C. Kurien, J. Chem. Soc. B 62 (1971) 2081.